HHS Public Access

Author manuscript

J Am Chem Soc. Author manuscript; available in PMC 2018 March 08.

Published in final edited form as:

J Am Chem Soc. 2017 March 08; 139(9): 3446–3455. doi:10.1021/jacs.6b11273.

Small Molecule Inhibition of microRNA-210 Reprograms an Oncogenic Hypoxic Circuit

Matthew G. Costales[†,⊥], **Christopher L. Haga**[‡,⊥], **Sai Pradeep Velagapudi**[†,⊥], **Jessica L. Childs-Disney**[†], **Donald G. Phinney**[‡], and **Matthew D. Disney**[*,†,§]

[†]Department of Chemistry, The Scripps Research Institute, 130 Scripps Way, Jupiter, Florida 33458, United States

[‡]Department of Molecular Therapeutics, The Scripps Research Institute, 130 Scripps Way, Jupiter, Florida 33458, United States

[§]Department of Neuroscience, The Scripps Research Institute, 130 Scripps Way, Jupiter, Florida 33458, United States

Abstract

A hypoxic state is critical to the metastatic and invasive characteristics of cancer. Numerous pathways play critical roles in cancer maintenance, many of which include noncoding RNAs such as microRNA (miR)-210 that regulates hypoxia inducible factors (HIFs). Herein, we describe the identification of a small molecule named Targapremir-210 that binds to the Dicer site of the miR-210 hairpin precursor. This interaction inhibits production of the mature miRNA, derepresses glycerol-3-phosphate dehydrogenase 1-like enzyme (GPD1L), a hypoxia-associated protein negatively regulated by miR-210, decreases HIF-1α, and triggers apoptosis of triple negative breast cancer cells only under hypoxic conditions. Further, Targapremir-210 inhibits tumorigenesis in a mouse xenograft model of hypoxic triple negative breast cancer. Many factors govern molecular recognition of biological targets by small molecules. For protein, chemoproteomics and activity-based protein profiling are invaluable tools to study small molecule target engagement and selectivity in cells. Such approaches are lacking for RNA, leaving a void in the understanding of its druggability. We applied Chemical Cross-Linking and Isolation by Pull Down (Chem-CLIP) to study the cellular selectivity and the on- and off-targets of Targapremir-210. Targapremir-210 selectively recognizes the miR-210 precursor and can differentially recognize RNAs in cells that have the same target motif but have different expression levels, revealing this important feature for selectively drugging RNAs for the first time. These studies show that small molecules can be rapidly designed to selectively target RNAs and affect cellular responses to environmental conditions, resulting in favorable benefits against cancer. Further, they help define rules for identifying druggable targets in the transcriptome.

[*] Disney@scripps.edu.

[⊥]Author Contributions

These authors contributed equally.

Supporting Information: The Supporting Information is available free of charge on the ACS Publications website at DOI: 10.1021/jacs.6b11273.

Supplementary figures and table, methods for chemical synthesis, nucleic acid binding assays, microarray analysis, ligand selectivity studies, and tumor localization (PDF)

The authors declare no competing financial interest.

Graphical abstract

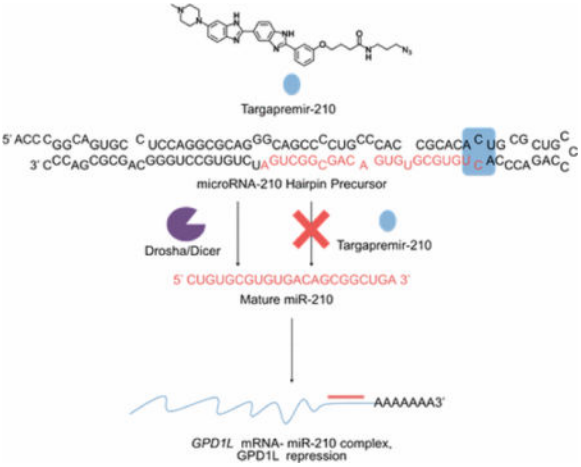

Introduction

RNA plays pervasive and important roles in cellular biology and can contribute to disease pathology. Although 80% of DNA is transcribed into RNA, only 1.5% is translated into protein.(1, 2) Not surprisingly, noncoding RNAs contribute to disease, cementing RNA as an important therapeutic target. Much effort has been invested in the development of small molecules targeting protein, however, the identification of small molecule modulators of RNA has only been sparsely reported. Thus, one long-standing challenge in drug discovery and chemical biology is selectively drugging human RNAs with small molecules.

To fill this void, we developed various synergistic approaches that enable the rational design of small molecules that target RNA from sequence. One foundational approach is Two-Dimensional Combinatorial Screening (2DCS), a library-versus-library screen that quickly defines the preferred RNA motifs for a given small molecule.(3) The data from 2DCS are compiled into a database that is mined against folded RNA structures within the human transcriptome to identify potentially druggable RNA targets from sequence via an approach named Inforna.(4, 5)

MicroRNAs (miRNAs) are one class of RNA drug targets that are at the forefront of drug discovery efforts. These small, noncoding RNAs negatively regulate protein expression by targeting the 3′ untranslated regions (UTRs) of mRNAs, leading to their translational repression or cleavage.(6–8) Numerous miRNAs are associated with disease pathology.(9) For example, microRNA (miR)-210 is a central regulator of the hypoxic response that affects expression of hypoxia inducible factors (HIFs) in solid tumor masses.(10) MiR-210 represses levels of the glycerol-3-phosphate dehydrogenase 1-like (GPD1L) enzyme, contributing to suppression of prolyl hydroxylase (PHD) activity.(10–12) Under normal physiological conditions, PHD hydroxylates prolines in hypoxia inducible factor 1-alpha (HIF-1α), leading to its degradation by the proteasome.(13) When PHD activity is suppressed due to downregulation of GPD1L by miR-210, HIF-1α is not degraded by the proteasome(10) and translocates to the nucleus where it forms a heterodimer with hypoxia-

inducible factor 1-beta (HIF-1β); dimerization of HIF-1α and HIF-1β activates transcriptional responses that contribute to cancer metastasis (Figure 1A).(14) Thus, small molecule inhibition of miR-210 could perturb this complex hypoxic circuit, leading to various favorable benefits for the treatment and study of cancer. Herein, we report that a small molecule *bis*-benzimidazole identified by Inforna,(4, 5) Targapremir-210 (Figure 1B), binds miR-210's Dicer processing site and modulates the miR-210 hypoxic circuit in triple negative breast cancer cells and a mouse xenograft model.

RESULTS and DISCUSSION

Biological Activity of Targapremir-210

We first assessed the ability of Targapremir-210 to inhibit Dicer processing of the miR-210 precursor (pre-miR-210) *in vitro*. As shown in Figure 2, Targapremir-210 inhibited pre-miR-210 processing at nanomolar concentrations, which correlated well with its binding affinity for the pre-miR-210 Dicer site, 5′A<u>C</u>U3′/3′U<u>C</u>A5′ (K_d ~ 200 nM).(15) Importantly, Targapremir-210 did not bind an RNA in which the Dicer site was ablated.(15) Targapremir-210 binds similarly to an *in vitro* transcribed pre-miR-210 (Figure S1A). Thus, Targapremir-210 bound avidly to pre-miR-210 and binding was sufficient to inhibit its processing *in vitro*.

To establish a cellular model to assess inhibition of miR-210 processing, we compared the expression profiles of various hypoxia-associated biomolecules in MDA-MB-231 triple negative breast cancer (TNBC) cells. As shown in Figure 3A, mature miR-210 levels were increased by 15-fold under hypoxic conditions, with similar effects observed for primary (pri-) and pre-miR-210. Concomitant changes were observed for *GPD1L* mRNA expression (10-fold reduction) and *HIF-1α* mRNA expression (10-fold increase) (Figure 3A), as expected.(10) Increased levels of *HIF-1α* and miR-210 have been previously observed in other breast cancer cell lines and in tissues.(13, 16, 17) Taken together, the MDA-MB-231 cell line serves as an appropriate model to study modulation of miR-210 by small molecules under hypoxic conditions.

In agreement with our *in vitro* studies demonstrating inhibition of pre-miR-210 Dicer processing by Targapremir-210 (Figure 2), the compound decreased mature miR-210 levels in MDA-MB-231 cells cultured under hypoxic conditions, with an IC_{50} of ~200 nM (Figure 3B). Concomitant increases were observed in pri- (~3-fold) and pre-miR-210 (~2.6-fold) levels upon treatment with 200 nM Targapremir-210 (Figure 3C), indicating that the compound's mode of action is inhibition of Dicer processing and not transcriptional silencing. An antagomir directed against miR-210, (anti-miR-210; 50 nM) decreased levels of the mature form of the miRNA but does not affect pri- and pre-miR-210 levels, as expected (Figure 3C).

Cellular Responses of Targapremir-210 in TNBC Cells

Given that Targapremir-210 decreases levels of mature miR-210, we studied the downstream cellular responses to Targapremir-210 treatment on MDA-MB-231 cells. As expected, *HIF-1α* mRNA levels in hypoxic MDA-MB-231 cells were reduced by ~75% following

treatment with 200 nM of Targapremir-210 whereas *GPD1L* mRNA levels were increased by ~4-fold, similar to the effects observed upon treatment with anti-miR-210 (Figure 3C). Thus, addition of the small molecule reverted the MDA-MB-231 genotypic expression levels toward that of a normoxic state, consistent with Targapremir-210 inhibiting miRNA biogenesis.

Under hypoxic conditions, upregulation of HIF-1α prevents cells from entering apoptosis.(18, 19) Because Targapremir-210 treatment reduced *HIF-1α* levels, we studied whether the compound could trigger apoptosis in MDA-MB-231 cells cultured under hypoxic conditions. Indeed, the compound induced apoptosis, as assessed by Annexin V/propidium iodide (PI) staining (Figure 4A). Furthermore, this response was selective for the hypoxic environment as Targapremir-210 did not induce apoptosis in MDA-MB-231 cells cultured in normoxia (Figure 4B). Notably, overexpression of pre-miR-210 allowed cells to escape apoptosis in the presence of the compound, suggesting that increased levels of the pre-miRNA overloaded the dosage of the compound (Figure 4A). Thus, the small molecule has desirable genotypic and phenotypic effects by inhibiting miR-210 biogenesis.

Cellular Selectivity: Hypoxia-Associated and off-target miRNAs

We next studied the cellular selectivity of Targapremir-210 and compared it with an antagomir directed against miR-210 by RT-qPCR. In particular, we analyzed the effect of compound treatment on a panel of hypoxia-associated miRNAs ($n = 28$).(20) Interestingly, both Targapremir-210 (200 nM) and anti-miR-210 (50 nM) affected only levels of mature miR-210, indicating that the compound is at least as selective as the oligonucleotide-based antagomir (Figure 5A).

To test further the selectivity of Taragpremir-210, we compared the effect of compound and miR-210 antagomir treatment using a microarray analysis of ~2500 miRNAs. Both the small molecule and antagomir had similar miRNA specificity profiles (Figure S2). These studies confirm the selectivity of Targapremir-210 is similar to that of a gene-specific antagomir on a transcriptome-wide level.

Cellular Selectivity: RNA Isoforms

There is extensive knowledge of protein isoform-specific targeting.(21, 22) Likewise, RNAs that have motifs that are recognized by the same small molecule represent, as we now term, RNA isoforms. One important feature of Inforna is its ability to identify privileged RNA motifs for a given small molecule and assign a Fitness Score to each (100 being the most fit) as a measure of selectivity.(4, 5) Indeed, a 2DCS selection of Targapremir-210 identified other small molecule-binding RNA motifs. Notably, these motifs have lower Fitness Scores and weaker affinities than the Dicer binding site in pre-miR-210.(15) We queried a database of secondary structural elements present in miRNA hairpin precursors(23) and identified miRNAs containing the pre-miR-210 Dicer site motif and other motifs that can bind to Targapremir-210, albeit with lower affinity (Table 1). Among all miRNAs with predicted compound binding sites, Targapremir-210 only affected levels of miR-210 (Figure 5B).

Direct Target Engagement of pre-miR-210 by Targapremir-210

To determine if Targapremir-210 directly engages the miR-210 hairpin precursor, we employed an approach developed in our laboratory named Chemical Cross-Linking and Isolation by Pull-Down (Chem-CLIP).(24) Briefly, a derivative of Targapremir-210 was synthesized that contains chlorambucil (CA) cross-linking and biotin purification modules (Targapremir-210-CA-Biotin; Figure 6A). Targapremir-210 drives binding to pre-miR-210, bringing chlorambucil into close proximity of the RNA such that they react to form a covalent cross-link. Biotin is then used to capture the cross-linked RNA on streptavidin beads. *In vitro* validation showed that the Targapremir-210 Chem-CLIP probe reacted selectively with pre-miR-210, as compared to the control Chem-CLIP compound without the RNA-binding module, which showed little to no reaction with the miR-210 precursor (Figure 6B).

In MDA-MB-231 cells grown under hypoxic conditions, Targapremir-210-CA-Biotin reacted with the miR-210 hairpin precursor, increasing the abundance of the target by greater than 20-fold in the purified fraction, when using primers that amplify only pre-miR-210 (Figure 6C). A competitive Chem-CLIP (C-Chem-CLIP) experiment was completed to assess if cross-linking of the target is due to nonspecific reactivity of the reactive (CA) module. In C-Chem-CLIP, cells are treated with the Chem-CLIP probe and increasing concentrations of the unreactive, parent compound. A target that binds selectively to the parent compound will be depleted as a function of concentration. A C-Chem-CLIP experiment completed in MDA-MB-231 cells showed that 200 nM of Targapremir-210 was required to inhibit ~50% of the reaction of Targapremir-210-CA-Biotin with pre-miR-210 (Figure 6C), which correlates well with the measured K_d of the compound with the pre-miR-210 Dicer site.

Direct Target Engagement of Highly Abundant Transcripts by Targapremir-210

To analyze the transcriptome-wide targets that Targapremir-210 engages in cells, we profiled the levels of 92 highly abundant transcripts in the pulled down fraction by Chem-CLIP. The RNAs analyzed included ribosomal (r)RNAs, small (s)RNAs, transfer (t)RNAs, and messenger (m)RNAs that span the diverse population of the transcriptome.(25) Among the 92 abundant transcripts, only six were present to a greater extent in the pulled-down fraction, with the largest relative pull-down equal to ~2-fold (Figure 7A,B); levels of mature miR-210 were enriched by greater than 7-fold. To determine if pull-down of the six enriched RNAs was due to nonselective binding caused by the chlorambucil and/or biotin modules, we completed a Chem-CLIP experiment with the Control-CA-Biotin compound (Figure 6A) that lacks the RNA-binding module. Interestingly, for three of the RNAs, there is no significant difference between the amount of RNA pulled down by Targapremir-210-CA-Biotin and Control-CA-Biotin (Figure S3A).

Direct Target Engagement of Hypoxia-Associated miRNAs by Targapremir-210

We also assessed the abundance of hypoxia-associated miRNAs in the pulled down fraction (Figure 7C). Indeed, miR-210 had the greatest abundance among the pulled down miRNAs by 1 order of magnitude. Enrichment was only observed for three of 28 of miRNAs studied (miR-181a, miR-205, and miR-206), with a highest relative fold pull-down of ~2.8-fold

(Figure 7C). To determine if enrichment might be caused by nonselective binding of the CA and biotin modules to the hypoxia-associated miRNAs, a C-Chem-CLIP experiment was completed. Compared to the C-Chem-CLIP results for miR-210, the abundance of other hypoxia-associated miRNAs did not change as a function of Targapremir-210 concentration, suggesting pull-down of these off-targets may be in part due to nonselective effects of the CA or biotin moieties (Figure S3B).

Direct Target Engagement of RNA Isoforms by Targapremir-210

We next determined if the 15 miRNAs that have an RNA isoform that binds Targapremir-210 are bound in MDA-MB-231 cells. By comparing the ability of Targapremir-210 to knock down mature levels of these miRNAs by RT-qPCR and to bind them by Chem-CLIP, we can assess: (i) if small molecules can differentially bind to RNAs that have the same RNA motif based on their expression level; (ii) if binding to nonfunctional sites (not Drosha and Dicer processing sites) has a biological effect; and (iii) other factors that can affect ligand occupancy of on- and off-targets.

Chem-CLIP studies revealed that only four of the miRNAs are bound by Targapremir-210 in MDA-MB-231 cells, miR-497, miR-1273c, miR-3174, and miR-107. Yet, the compound has no statistically significant effect on any of their expression levels. Interestingly, miR-497 contains the exact same motif as miR-210's Dicer site but the motif is located outside Dicer or Drosha processing sites. Further, miR-497 levels are 10-fold lower than miR-210, which is reflective of its decreased enrichment as compared to miR-210. A Targapremir-210 binding site is present in the Dicer or Drosha processing sites of miR-324, miR-3174, and miR-4446. All three miRNAs are lower abundance as compared to miR-210 (at least 2-fold) and their predicted binding sites are >10-fold less avid than miR-210's Dicer site.

The cellular occupancy of miR-1273c by Targapremir-210 is an interesting case, as the same motif (5′C<u>C</u>U/3′G<u>A</u>A) that binds the compound is present in four miRNAs that were not enriched in Chem-CLIP studies, miR-648, miR-103a, miR-4682, and miR-3120. MiR-648 and miR-3120 are expressed at much lower levels than miR-1273c (>10-fold), which could explain why they are not occupied *in cellulis*. In contrast, miR-103a abundance is similar to miR-1273c's while miR-4682 is 2-fold higher. Careful inspection of miR-1273c's secondary structure provides potential insight into its greater occupancy by Targapremir-210 as compared to miR-103a and miR-4682: its secondary structure contains three CA internal loop motifs that could be bound by Targapremir-210.

Collectively, these data suggest that (i) simple binding is not sufficient to elicit a biological effect; rather, binding must occur to a functional (Dicer or Drosha processing) site; (ii) the compound must bind avidly to a processing site; and (iii) the degree of target occupancy depends on the abundance of the RNA and the affinity of the small molecule.

The Chem-CLIP approach also has implications for determining RNA secondary structure. Chemical modification reagents such as dimethyl sulfate (DMS)(26–28) and Selective 2′-Hydroxyl Acylation and Primer Extension (SHAPE) reagents(29, 30) have provided invaluable tools to constrain RNA structure predictions from sequence. Likewise, the

observation that small molecules recognize specific RNA motifs in cells could provide invaluable constraints to refine cellular RNA structures.

Targapremir-210 as an RNA-Binding Module

Interestingly, Targaprimir-96,(4) a dimer that selectively targets pri-miR-96, displays Targapremir-210 as one of its RNA-binding modules. Thus, we tested if Targaprimir-96 affects miR-210 levels and if Targapremir-210 affects miR-96 levels under hypoxic conditions. Importantly, we found that Targaprimir-96 only affects miR-96 and that Targapremir-210 only affects miR-210 (Figure S4). Thus, molecular recognition in cells is governed by the RNA-binding module in the context of the entire ligand. Such properties have been shown previously.(31, 32)

Pharmacological Testing of Targapremir-210

Previously, compounds within the *bis*-benzimidazole class have been used as topoisomerase inhibitors.(33) Topoisomerases catalyze the breakage and rejoining of the DNA backbone, and topoisomerase inhibitors are known to be efficient inducers of apoptosis.(34) Thus, we tested if Targapremir-210 inhibited topoisomerase enzymatic activity *in vitro*. At 200 nM, the active concentration used in our TNBC cell studies, Targapremir-210 did not inhibit topoisomerase activity (Figure S5), suggesting that it triggers apoptosis in TNBC cells via on-target inhibition of miR-210 biogenesis, in agreement with RT-qPCR data that showed increases in pri- and pre-miR-210 levels (Figure 3C) and the loss of compound activity upon overexpression of pre-miR-210 (Figure 4B).

Other *bis*-benzimidazoles are currently used as fluorescent stains for DNA, such as Hoechst 33342. Hoechst 33342 is structurally similar to Targapremir-210 except the former phenol is *para* substituted as opposed to *meta* substituted. Therefore, we measured the affinity of Hoechst 33342 for pre-miR-210. No saturable binding was observed when up to 5000 nM pre-miR-210 was added, indicating that it binds much less avidly than Targapremir-210 (Figure S1). Similarly, Hoechst 33342 (200 nM; approximate IC_{50} of Targapremir-210) has no statistically significant effect on mature miR-210 levels in hypoxic MDA-MB-231 cells (Figure S6).

Targapremir-210 Decreases Tumor Burden in a TNBC Mouse Model

Because of the favorable functional consequences and selectivity of Targapremir-210, we completed *in vivo* studies of hypoxic breast cancer tumor burden. In these studies, MDA-MB-231 cells that stably express luciferase, MDA-MB-231-GFP-Luc, were generated and used for tumor implantation. MDA-MB-231-GFP-Luc cells were pretreated with Targapremir-210 (200 nM) or anti-miR-210 antagomir (500 nM) and then implanted into mammary fat pads. Alternatively, MDA-MB-231-GFP-Luc were implanted into fat pads and mice were treated with Targapremir-210 (200 nM) or anti-miR-210 antagomir (500 nM) 24 h later with a single *i.p.* injection. After 21 days, tumor burden was assessed by live bioluminescent imaging. Both anti-miR-210 and Targapremir-210 significantly decreased tumor growth as assessed by luciferase signal intensity (Figure 8A) and mass of the resected tumor (Figure 8B). Fluorescent microscopy was used to visualize compound localization and

showed that a single *i.p.* injection of Targapremir-210 was able to reach the tumor and sustain for the entire 21-day period (Figure S7).

The resected tumors were assessed for perturbation in the hypoxic signaling pathway upon compound treatment by RT-qPCR. Tumors treated with both the antagomir and Targapremir-210 expressed significantly lower levels of miR-210 and *HIF-1α* mRNA and significantly higher levels of *GPD1L* mRNA as compared to untreated tumors (Figure 8C). Specifically, Targapremir-210 treatment reduced miR-210 and *HIF-1α* levels by ~90% and ~75%, respectively, compared to untreated tumors, whereas *GPD1L* levels were doubled. These results demonstrate that Targapremir-210 modulated its intended target (miR-210) *in vivo* and disrupted adaptive responses to hypoxia that promote tumor growth.

Conclusions and Implications

In summary, these studies showed that small molecules can have cell type-specific effects by targeting noncoding RNAs and can also selectively target RNAs based on differential environmental conditions. The bioactivity of Targapremir-210 in TNBC cells and in a mouse tumor model demonstrated how RNA-binding small molecules can effectively probe a complex hypoxic circuit and potentially be developed into cancer therapeutics. Importantly, studies with the Targapremir-210 Chem-CLIP probe determined that RNA-binding small molecules can engage the desired RNA target even among other abundant transcripts. Furthermore, an emerging encyclopedia of information suggests that RNAs that fold into defined secondary structures but have limited tertiary structure can indeed be targeted with small molecules.(4, 35, 36)

These studies validate that small molecules targeting RNA structure is a viable strategy to modulate the dysfunction of disease-associated RNAs. They also elucidate that small molecules must target a functional site to obtain a bioactive interaction for RNA. Most importantly, expression levels of different RNAs are a driver of ligand occupancy in cells. RNAs with higher expression levels are more likely to be occupied by a small molecule. Taken together, RNA may be more druggable with small molecules than anticipated.

Experimental Methods

PCR Amplification and in Vitro Transcription

The DNA template for the miR-210 precursor (5′-AGCCCCTGCCCACCGCACACTGCGCTGCCCCAGACCCACTGTGCGTGTGA-CAGCGGCTGA) was purchased from Eurofins MWG Operon and used without further purification. This template was PCR amplified in 1× PCR Buffer (10 mM Tris, pH 9.0, 50 mM KCl, and 0.1% (v/v) Triton X-100), 2 μM forward primer (5′-TAATACGACTCACTATAGGAGCCCCTGCCCACCGCACAC), 2 μM reverse primer (5′-TCAGCCGCTGTCACACGCACA), 4.25 mM $MgCl_2$, 330 μM dNTPs, and 1 μL of Taq DNA polymerase in a 600 μL reaction. PCR cycling conditions were 95 °C for 30 s, 50 °C for 30 s, and 72 °C for 60 s.

RNA was *in vitro* transcribed by T7 RNA polymerase in 1× Transcription Buffer (40 mM Tris–HCl, pH 8.1, 1 mM spermidine, 0.001% (v/v) Triton X-100 and 10 mM DTT) with

2.25 mM of each rNTP and 5 mM $MgCl_2$ at 37 °C for 18 h. The RNA was then purified on a denaturing 15% polyacrylamide gel and isolated as previously described.(4) RNA concentration was determined by UV absorbance at 260 nm at 90 °C using a Beckman Coulter DU800 UV–vis spectrophotometer with a Peltier temperature controlling unit. Extinction coefficients were calculated using the Oligo Extinction Coefficient Calculator (https://www.scripps.edu/california/research/dna-protein-research/forms/biopolymercalc2.html).

In Vitro Dicer Protection Assay

The miR-210 precursor was 5′-end labeled with [γ-^{32}P] ATP and T4 polynucleotide kinase as previously described.(4) The RNA was then folded in 1× Reaction Buffer (Genlantis) by heating at 60 °C for 5 min and slowly cooling to room temperature, where it was then supplemented with 1 mM ATP and 2.5 mM $MgCl_2$. Targapremir-210 was added to the reaction mixture and the samples were allowed to incubate at room temperature for 15 min. Recombinant human Dicer enzyme (Genlantis) was added to a final concentration of 0.01 U/μL and the samples were incubated for an additional 30 min at 37 °C. Reactions were stopped by adding in 2× Gel Loading Buffer (8 M urea, 50 mM EDTA, 0.05% (w/v) bromophenol blue, 0.05% (w/v) xylene cyanol). To generate sequencing markers, pre-miR-210 was digested with RNase T1 (0.125 U/μL) in T1 Buffer (25 mM sodium citrate, pH 5, 7 M urea, and 1 mM EDTA) for 20 min at room temperature. An RNA hydrolysis ladder was prepared by incubating RNA in 1× RNA Hydrolysis Buffer (50 mM $NaHCO_3$, 1 mM EDTA, pH 9.4) at 95 °C for 5 min. Cleavage products were resolved on a denaturing 15% polyacrylamide gel, which was imaged using a Molecular Dynamics Typhoon phosphorimager and quantified with Bio-Rad's QuantityOne software.

Cell Culture

MDA-MB-231 cells were cultured in RPMI 1640 medium supplemented with 10% FBS (Sigma), 1× Glutagro (Corning), and 1× Pen/Strep (MP Biomedicals, LLC) (growth medium). Cells cultured in normoxia were maintained at 37 °C in ambient atmosphere (~21% O_2) with 5% CO_2. Cells cultured in hypoxia were maintained at 37 °C, < 1% O_2 in a nitrogen filled hypoxic chamber (Billups-Rothenberg, Inc.), and 5% CO_2.

RNA Isolation and RT-qPCR

Total RNA was extracted from cells using a Quick-RNA MiniPrep Kit (Zymo Research) per the manufacturer's protocol. Approximately 200–600 ng of RNA was used in subsequent reverse transcription reactions using a miScript II RT Kit (Qiagen) or a qScript cDNA Synthesis Kit (Quanta Biosciences) per the manufacturers' recommended protocols. Primers for RT-qPCR were purchased from Integrated DNA Technologies (IDT) or Eurofins (Table S1) and used without further purification. RT-qPCR samples were prepared using Power SYBR Green PCR Master Mix (Applied Biosystems) and completed by using a 7900HT Fast Real Time PCR System (Applied Biosystems). Expression levels of RNAs were normalized to U6 small nuclear RNA, *GAPDH* mRNA, or 18S rRNA.

In Vitro Chem-CLIP

Growth medium was inactivated by heating at 95 °C for 15 min and then cooling to room temperature. Approximately 10000 counts of miR-210 precursor 5′-end labeled with ^{32}P was added and folded at 60 °C for 5 min. After cooling, dilutions of Targapremir-210-CA-Biotin or Control CA-Biotin were added and incubated at 37 °C overnight. A 300 μL slurry of streptavidin-agarose beads (Sigma-Aldrich) was washed three times with 1× PBS and resuspended in 1× PBS. A 20 μL aliquot of the slurry was then added to the samples, which were incubated for 1 h at room temperature. The samples were centrifuged and the supernatant containing unbound RNA was transferred to a new tube. The beads were then washed three times with 1× PBS supplemented with 0.1% (v/v) Tween-20 and centrifuged, with each wash supernatant being added to the tube containing unbound RNA. The amounts of radioactivity in the supernatant and on the beads were quantified with a Beckman Coulter LS6500 Liquid Scintillation Counter.

Cellular Chem-CLIP and C-Chem-CLIP

MDA-MB-231 cells were grown in growth medium as monolayers in 60 mm dishes to ~60% confluency. For Chem-CLIP studies, cells were then treated with 200 nM of Targapremir-210-CA-Biotin or Control CA-Biotin; for C-Chem-CLIP studies, cells were treated with 200 nM Targapremir-210-CA-Biotin and increasing concentrations of the parent Targapremir-210 compound. Cells were immediately placed under hypoxic conditions for 48 h, and total RNA was extracted using a Quick-RNA MiniPrep Kit (Zymo Research) per the manufacturer's protocol. Approximately 10 μg of total RNA was incubated with 100 μL of streptavidin-agarose beads in 1× PBS for 1 h at room temperature with gentle shaking. The solution was removed and the beads were washed 8 times with 300 μL of 1× PBS. Bound RNA was released from the beads by heating in 1× Elution Buffer (95% formamide, 10 mM EDTA, pH 8.2) at 60 °C for 20 min. The pulled-down RNA was purified using a Quick-RNA MiniPrep Kit (Zymo Research) and then used for subsequent RT and qPCR reactions as described above.

The relative fold-change in the amount of an RNA before and after pull-down was calculated by the $\Delta\Delta C_t$ method as shown in eq 1:

$$\text{Relative Fold} - \text{Change:} 2^{-(\Delta C_t \text{before pull- down} - \Delta C_t \text{after pull- down})} \quad (1)$$

where the "ΔC_t before pull-down" is the difference between the C_t values for the RNA of interest and a housekeeping gene (U6 small nuclear RNA, *GAPDH* mRNA, or 18S rRNA) in total RNA isolated from cells and "ΔC_t after pull-down" is the difference between the C_t values for the RNA of interest and the same housekeeping gene after pull-down.

In Vitro Topoisomerase Inhibition Assay

Topoisomerase II inhibitory activity was measured using a Topoisomerase II Drug Screening Kit (TopoGEN, Inc.) per the manufacturer's protocol. Taragpremir-210 (200 nM) was added to 300 ng of DNA in 1× Complete Buffer (50 mM Tris–HCl, pH 8, 150 mM NaCl, 10 mM $MgCl_2$, 0.5 mM dithiothreitol, 30 μg/mL BSA, and 2 mM ATP), followed by addition of 7.5

U of Topoisomerase II enzyme. The samples were incubated for 30 min at 37 °C, and the reaction was stopped by the addition of 2 μL of 10% sodium dodecyl sulfate (SDS). Proteinase K (50 μg/mL) was then added and the solution was incubated for 15 min at 37 °C. Topoisomers were separated on 1% agarose gels with or without 0.5 μg/mL ethidium bromide. Note, for gels containing ethidium bromide, the 1× TAE running buffer was also supplemented with 0.5 μg/mL ethidium bromide. Gels prepared without ethidium bromide were poststained (0.5 μg/mL ethidium bromide). Both types of gels were destained in 1× TAE for 15 min, and the DNA products were visualized using a Bio-Rad Gel Doc XR+ imaging system.

Mice

NOD/SCID mice (B6.CB17-Prkdcscid/Sz, Jackson Laboratories) were housed in the Scripps Florida vivarium. All live animal experiments were approved by the Scripps Florida Institutional Animal Care and Use Committee. Two sets of experiments were completed: treatment of MDA-MB-231-GFP-luc cells prior to implantation and treatment of mice post-tumor implantation. For pretreatment of tumor cells, MDA-MB-231-GFP-luc cells (5×10^6) were treated with or without Targapremir-210 (200 nM) or anti-miR-210 antagomir (500 nM) for 48 h preimplantation. A 100 μL PBS/Matrigel (1:1; BD Biosciences) cell suspension was subcutaneously transplanted into mouse breast fat pads. Alternatively, mouse breast fat pads were injected with a 100 μL PBS/Matrigel (1:1) cell suspension (5×10^6 MDA-MB-231-GFP-luc cells) followed by intraperitoneal (*i.p.*) injection of Targapremir-210 (100 μL of 200 nM) or anti-miR-210 antagomir (100 μL of 500 nM) 24 h post-transplantation.

Tumor growth was monitored weekly postimplantation by *i.p.* injection of 200 μL D-luciferin (15 mg/mL) and imaging with an IVIS 200 system. Tumors were resected 21 days post-transplantation following euthanasia. Levels of mature miR-210, *HIF-1α*, and *GPD1L* RNAs were measured by RT-qPCR as described above.

Supplementary Material

Refer to Web version on PubMed Central for supplementary material.

Acknowledgments

This work was funded by the Scheller Graduate Student Fellowship to M.G.C. and the National Institutes of Health (R01GM97455 to M.D.D.).

References

1. Gerstein MB, Bruce C, Rozowsky JS, Zheng D, Du J, Korbel JO, Emanuelsson O, Zhang ZD, Weissman S, Snyder M. Genome Res. 2007; 17:669.doi: 10.1101/gr.6339607 [PubMed: 17567988]
2. Clamp M, Fry B, Kamal M, Xie X, Cuff J, Lin MF, Kellis M, Lindblad-Toh K, Lander ES. Proc Natl Acad Sci U S A. 2007; 104:19428.doi: 10.1073/pnas.0709013104 [PubMed: 18040051]
3. Childs-Disney JL, Wu M, Pushechnikov A, Aminova O, Disney MD. ACS Chem Biol. 2007; 2:745.doi: 10.1021/cb700174r [PubMed: 17975888]
4. Velagapudi SP, Gallo SM, Disney MD. Nat Chem Biol. 2014; 10:291.doi: 10.1038/nchembio.1452 [PubMed: 24509821]

5. Disney MD, Winkelsas AM, Velagapudi SP, Southern M, Fallahi M, Childs-Disney JL. ACS Chem Biol. 2016; 11:1720.doi: 10.1021/acschembio.6b00001 [PubMed: 27097021]
6. He L, Hannon GJ. Nat Rev Genet. 2004; 5:522.doi: 10.1038/nrg1379 [PubMed: 15211354]
7. Bartel DP. Cell. 2004; 116:281.doi: 10.1016/S0092-8674(04)00045-5 [PubMed: 14744438]
8. Behm-Ansmant I, Rehwinkel J, Izaurralde E. Cold Spring Harbor Symp Quant Biol. 2006; 71:523.doi: 10.1101/sqb.2006.71.013 [PubMed: 17381335]
9. Bartel DP. Cell. 2009; 136:215.doi: 10.1016/j.cell.2009.01.002 [PubMed: 19167326]
10. Kelly TJ, Souza AL, Clish CB, Puigserver P. Mol Cell Biol. 2011; 31:2696.doi: 10.1128/MCB.01242-10 [PubMed: 21555452]
11. Redova M, Poprach A, Besse A, Iliev R, Nekvindova J, Lakomy R, Radova L, Svoboda M, Dolezel J, Vyzula R, Slaby O. Tumor Biol. 2013; 34:481.doi: 10.1007/s13277-012-0573-2
12. Grosso S, Doyen J, Parks SK, Bertero T, Paye A, Cardinaud B, Gounon P, Lacas-Gervais S, Noel A, Pouyssegur J, Barbry P, Mazure NM. Mari BCell Death Dis. 2013; 4:e544.doi: 10.1038/cddis.2013.71
13. Maxwell PH, Wiesener MS, Chang GW, Clifford SC, Vaux EC, Cockman ME, Wykoff CC, Pugh CW, Maher ER, Ratcliffe PJ. Nature. 1999; 399:271.doi: 10.1038/20459 [PubMed: 10353251]
14. Semenza GL. Nat Rev Cancer. 2003; 3:721.doi: 10.1038/nrc1187 [PubMed: 13130303]
15. Velagapudi SP, Seedhouse SJ, French J, Disney MD. J Am Chem Soc. 2011; 133:10111.doi: 10.1021/ja200212b [PubMed: 21604752]
16. Rothé F, Ignatiadis M, Chaboteaux C, Haibe-Kains B, Kheddoumi N, Majjaj S, Badran B, Fayyad-Kazan H, Desmedt C, Harris AL, Piccart M, Sotiriou C. PLoS One. 2011; 6:e20980.doi: 10.1371/journal.pone.0020980 [PubMed: 21738599]
17. Blancher C, Moore JW, Talks KL, Houlbrook S, Harris AL. Cancer Res. 2000; 60:7106. [PubMed: 11156418]
18. Greijer AE, van der Wall EJ. Clin Pathol. 2004; 57:1009.doi: 10.1136/jcp.2003.015032
19. Kilic M, Kasperczyk H, Fulda S, Debatin KM. Oncogene. 2007; 26:2027.doi: 10.1038/sj.onc.1210008 [PubMed: 17043658]
20. Kulshreshtha R, Ferracin M, Wojcik SE, Garzon R, Alder H, Agosto-Perez FJ, Davuluri R, Liu C-G, Croce CM, Negrini M, Calin GA, Ivan M. Mol Cell Biol. 2007; 27:1859.doi: 10.1128/MCB.01395-06 [PubMed: 17194750]
21. Alterio V, Di Fiore A, D'Ambrosio K, Supuran CT, De Simone G. Chem Rev. 2012; 112:4421.doi: 10.1021/cr200176r [PubMed: 22607219]
22. Thorpe LM, Yuzugullu H, Zhao JJ. Nat Rev Cancer. 2015; 15:7.doi: 10.1038/nrc3860 [PubMed: 25533673]
23. Liu B, Childs-Disney JL, Znosko BM, Wang D, Fallahi M, Gallo SM, Disney MD. BMC Bioinformatics. 2016; 17:1.doi: 10.1186/s12859-016-0960-6 [PubMed: 26817711]
24. Guan L, Disney MD. Angew Chem Int Ed Engl. 2013; 52:10010.doi: 10.1002/anie.201301639 [PubMed: 23913698]
25. Yang W-Y, Gao R, Southern M, Sarkar PS, Disney MD. Nat Commun. 2016; 7:11647.doi: 10.1038/ncomms11647 [PubMed: 27248057]
26. Mathews DH, Disney MD, Childs JL, Schroeder SJ, Zuker M, Turner DH. Proc Natl Acad Sci U S A. 2004; 101:7287.doi: 10.1073/pnas.0401799101 [PubMed: 15123812]
27. Wells SE, Hughes JM, Haller AI, Ares M Jr. Methods Enzymol. 2000; 318:479.doi: 10.1016/S0076-6879(00)18071-1 [PubMed: 10890007]
28. Kwok CK, Ding Y, Tang Y, Assmann SM, Bevilacqua PC. Nat Commun. 2013; 4:2971.doi: 10.1038/ncomms3971 [PubMed: 24336128]
29. Spitale RC, Crisalli P, Flynn RA, Torre EA, Kool ET, Chang HY. Nat Chem Biol. 2013; 9:18.doi: 10.1038/nchembio.1131 [PubMed: 23178934]
30. Deigan KE, Li TW, Mathews DH, Weeks KM. Proc Natl Acad Sci U S A. 2009; 106:97.doi: 10.1073/pnas.0806929106 [PubMed: 19109441]
31. Lee MM, Childs-Disney JL, Pushechnikov A, French JM, Sobczak K, Thornton CA, Disney MD. J Am Chem Soc. 2009; 131:17464.doi: 10.1021/ja906877y [PubMed: 19904940]

32. Childs-Disney JL, Tsitovich PB, Disney MD. ChemBioChem. 2011; 12:2143.doi: 10.1002/cbic.201100298 [PubMed: 21830289]
33. Beerman TA, McHugh MM, Sigmund R, Lown JW, Rao KE, Bathini Y. BBA – Gene Struct Expr. 1992; 1131:53.doi: 10.1016/0167-4781(92)90098-K
34. Nitiss JL. Nat Rev Cancer. 2009; 9:338.doi: 10.1038/nrc2607 [PubMed: 19377506]
35. Velagapudi SP, Cameron MD, Haga CL, Rosenberg LH, Lafitte M, Duckett DR, Phinney DG, Disney MD. Proc Natl Acad Sci U S A. 2016; 113:5898.doi: 10.1073/pnas.1523975113 [PubMed: 27170187]
36. Kumar A, Parkesh R, Sznajder LJ, Childs-Disney JL, Sobczak K, Disney MD. ACS Chem Biol. 2012; 7:496.doi: 10.1021/cb200413a [PubMed: 22252896]

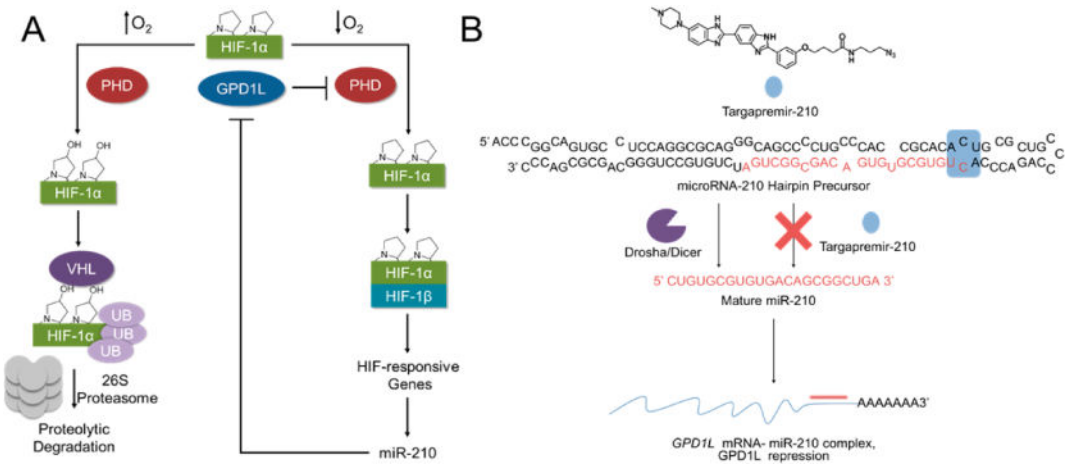

Figure 1.

Overview of miR-210 and Targapremir-210 activity. (A) Schematic of miR-210's regulatory effect on GPD1L and HIF-1α in hypoxia, which contributes to the metastasis of cancer cells. GPD1L, glycerol-3-phosphate dehydrogenase 1-like enzyme; HIF-1α, hypoxia-inducible factor 1-alpha; HIF-1β, hypoxia-inducible factor 1-beta; PHD, prolyl hydroxylase; UB, ubiquitin; VHL, Von Hippel—Lindau tumor suppressor (E3 ubiquitin protein ligase). (B) Schematic of an approach to inhibit miR-210 biogenesis with a designed small molecule, Targapremir-210.

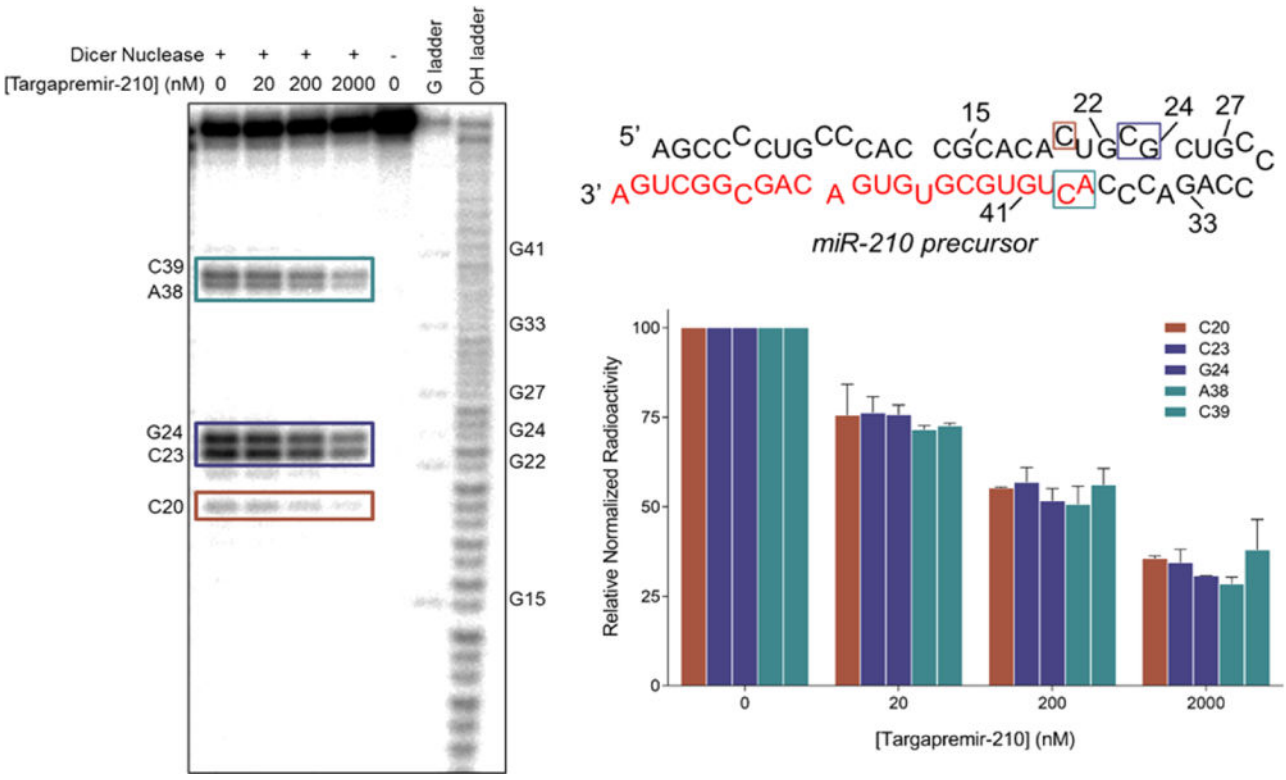

Figure 2.

Targapremir-210 inhibits processing of pre-miR-210 by Dicer *in vitro.* (Left) Representative gel image of the inhibition of pre-miR-210 processing by Dicer as a function of Targapremir-210 concentration. Nucleotides protected from Dicer cleavage are boxed and indicated in miR-210's secondary structure (Right, top). A "G ladder" was generated by digestion with RNase T1; "OH ladder" indicates a base hydrolysis ladder. (Right) Secondary structure of pre-miR-210 and quantification of protection from Dicer cleavage. Nucleotides protected from Dicer cleavage are boxed in the secondary structure.

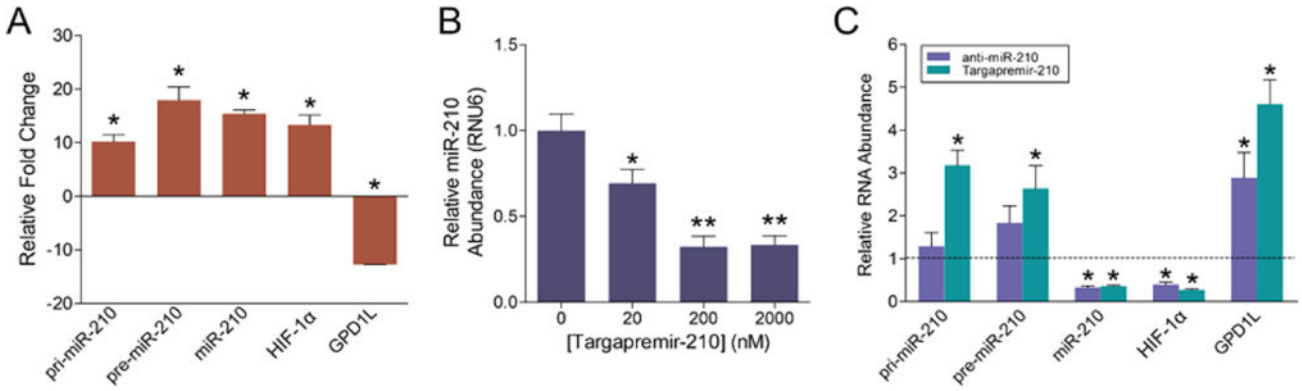

Figure 3.

Biological activity of Targapremir-210. (A) Expression of various RNAs in MDA-MB-231 cells under hypoxic conditions, showing increased levels of pri-, pre-, and mature miR-210 and *HIF-1α* and decreased levels of *GPD1L.* *, $p < 0.05$ compared to normoxic expression, as determined by a two tailed Student *t* test. (B) Effect of Targapremir-210 on levels of mature miR-210 in MDA-MB-231 cells cultured under hypoxic conditions, as determined by RT-qPCR *, $p < 0.05$ and **, $p < 0.01$ compared to untreated, as determined by a two-tailed Student *t* test. (C) Effect of Targapremir-210 (200 nM) and an antagomir directed against miR-210 (50 nM) on pri- and pre-miR-210, *HIF-1α*, and *GPD1L* levels in MDA-MB-231 cells as determined RT-qPCR The dashed line represents no change in RNA levels as compared to untreated MDA-MB-231 cells. *, $p < 0.05$ compared to untreated, as determined by a two-tailed Student *t* test.

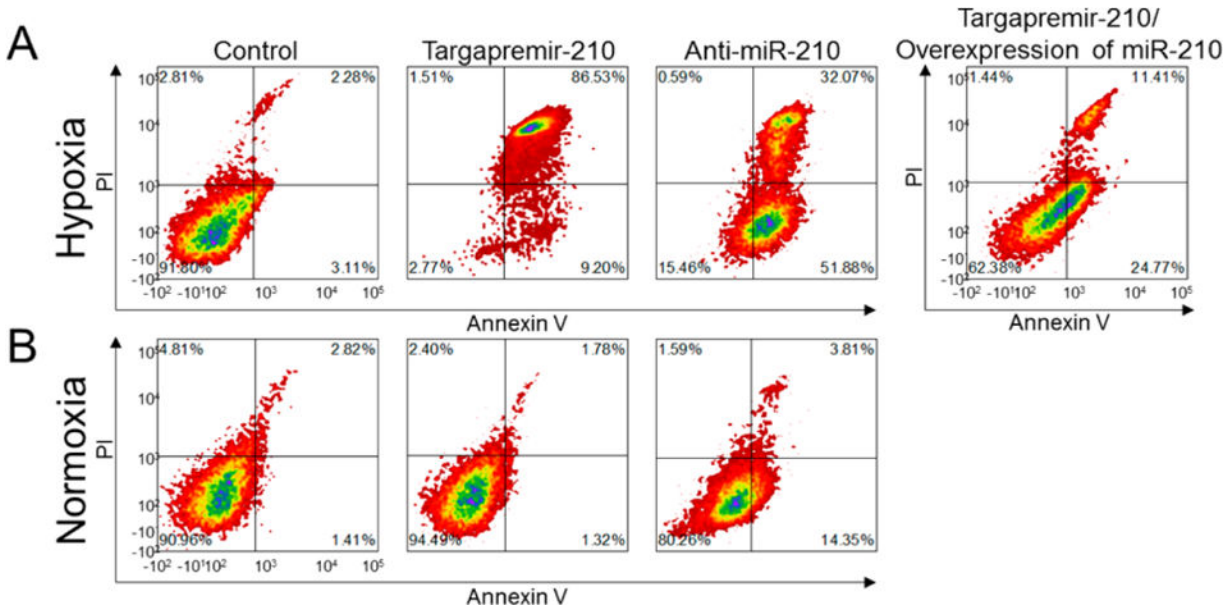

Figure 4.

Effect of Targapremir-210 or anti-miR-210 antagomir on MDA-MB-231 cell survival in hypoxia or normoxia. (A) Targapremir-210 (200 nM) and an antagomir directed against miR-210 (anti-miR-210; 50 nM) trigger apoptosis in MDA-MB-231 cells cultured under hypoxic conditions, as determined by Annexin V/PI staining and analysis by flow cytometry. Overexpression of pre-miR-210 ablated the ability of Targapremir-210 to trigger apoptosis. (B) Targapremir-210 (200 nM) and anti-miR-210 (50 nM) do not trigger apoptosis in MDA-MB-231 cells cultured in normoxic conditions, as determined by Annexin V/PI staining and analysis by flow cytometry.

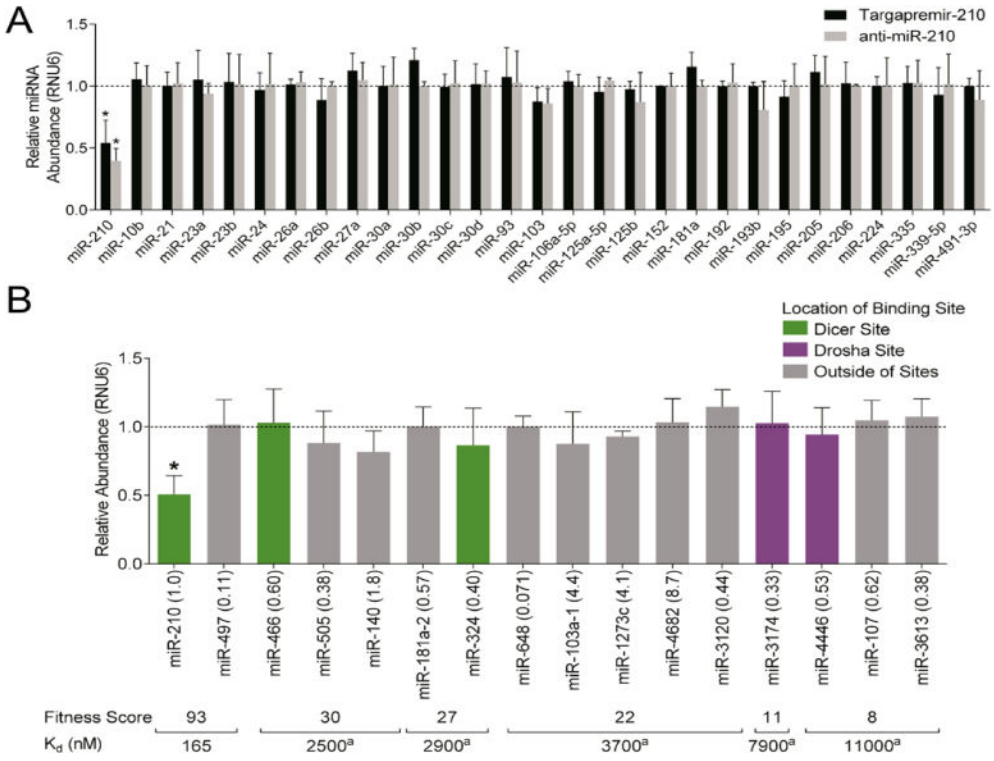

Figure 5.

Cellular selectivity of Targapremir-210 in MDA-MB-231 cells. (A) Among miRNAs upregulated in MDA-MB-231 cells under hypoxic conditions, miR-210 is the only one significantly affected by Targapremir-210 (200 nM), with a similar signature as an antagomir (50 nM), as determined by RT-qPCR The dashed line represents no change in RNA levels as compared to untreated MDA-MB-231 cells. (B) Among miRNAs that contain motifs that bind Targapremir-210 with various affinities, only miR-210 expression levels are affected by the compound in MDA-MB-231 cells cultured under hypoxic conditions, as determined by RT-qPCR. The value indicated in parentheses after the miRNA identifier indicates its normalized expression level, as compared to miR-210, in untreated cells. [a]Predicted affinity; [15] *, $p < 0.05$ as determined by a two-tailed Student *t* test.

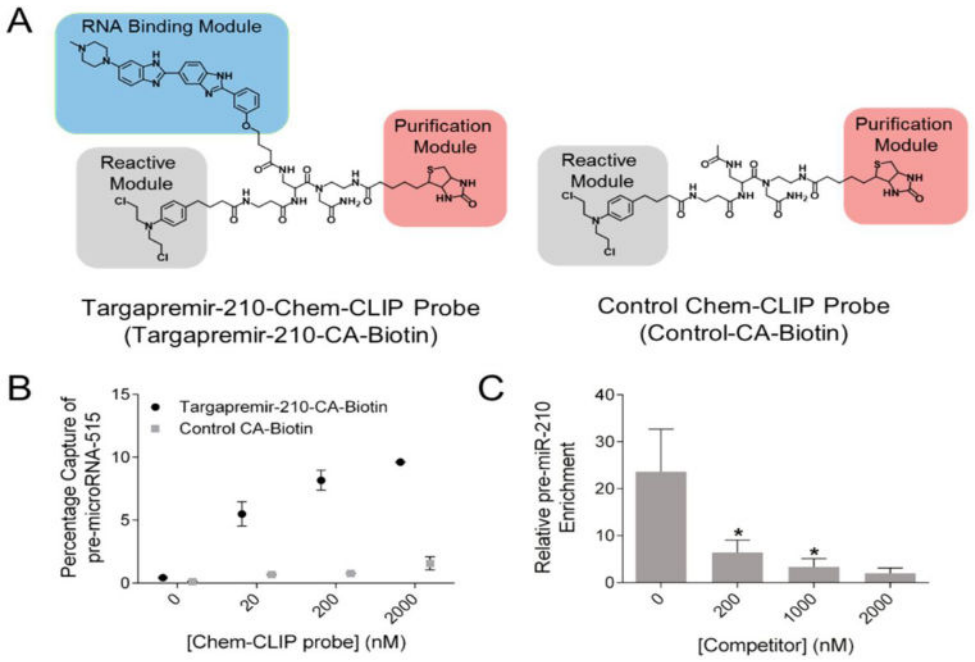

Figure 6.

Evaluation of Targapremir-210 target engagement. (A) Structures of small molecules used to study Targapremir-210 target engagement via Chemical Cross-Linking and Isolation by Pull Down (Chem-CLIP). The control Chem-CLIP probe, Control-CA-Biotin, lacks an RNA-binding module. (B) *In vitro* experiments show that the Targapremir-210-CA-Biotin Chem-CLIP probe selectively binds pre-miR-210 as compared to a CA-biotin probe lacking the RNA-binding module (Control-CA-Biotin). (C) Treatment of MDA-MB-231 cells with Targapremir-210-CA-Biotin affords ~20-fold enrichment of pre-miR-210 in the pulled down fraction, indicating reaction with the RNA in cells. Addition of Targapremir-210 inhibits reaction of Targapremir-210-CA-Biotin with pre-miR-210, indicating on-target effects of the probe and the designed small molecule. *, $p < 0.05$ as determined by a two-tailed Student *t* test.

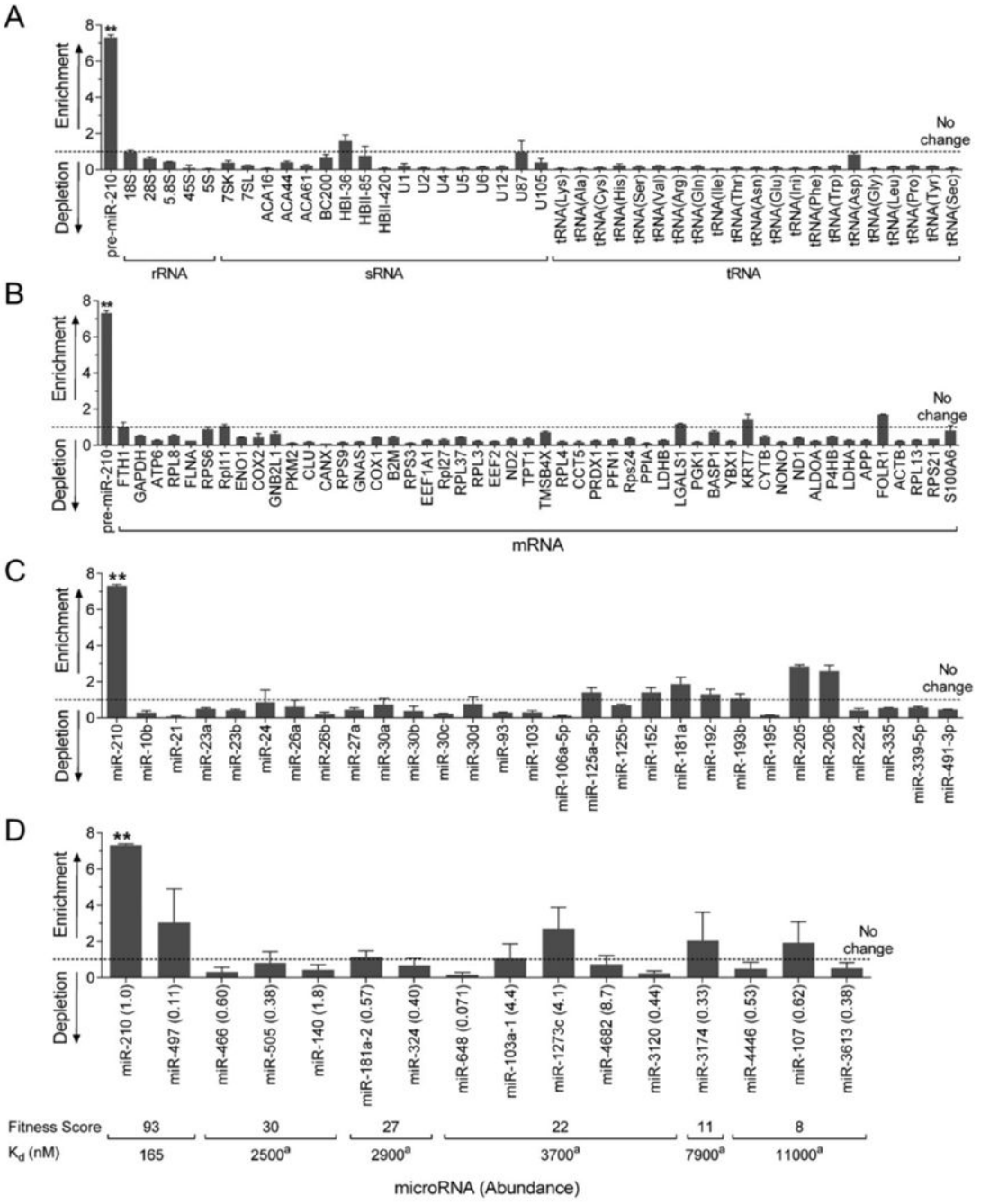

Figure 7.

Cellular selectivity of Targapremir-210. (A, B) Relative fold enrichment of abundant human RNAs in MDA-MB-231 cells cultured under hypoxic conditions following Targapremir-210-CA-Biotin pulldown via Chem-CLIP. (C) Relative fold enrichment of hypoxia-associated miRNAs as determined by Chem-CLIP. (D) Relative fold enrichment of miRNAs that contain a binding site for Targapremir-210 with varying affinities and expression levels, as determined by Chem-CLIP. [a]Predicted affinity;[15] **, $p < 0.01$, as determined by a two-tailed Student *t* test.

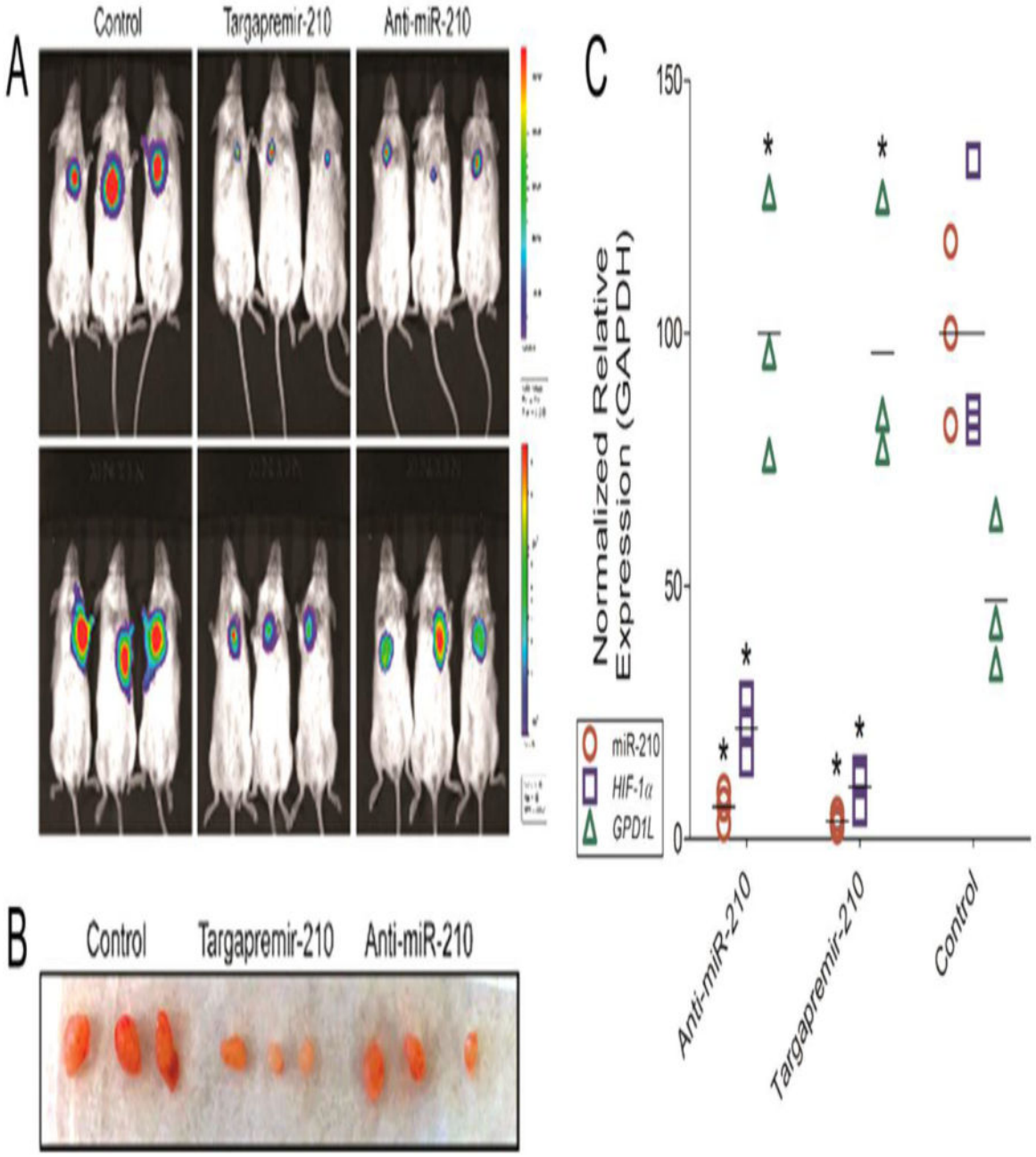

Figure 8.

Targapremir-210 impedes tumor proliferation *in vivo.* (A) Live bioluminescent imaging of NOD/SCID mice 3 weeks postimplantation of MDA-MB-231-GFP-Luc cells either pretreated *in vitro* with Targapremir-210 or miR-210 antagomir (top) or administered with a single injection of Targapremir-210 or miR-210 antagomir 24 h postimplantation (bottom). (B) Resected tumor masses from NOD/SCID mice administered with a single injection of either Targapremir-210 or miR-210 antagomir 24 h post tumor implantation. (C) Real-time qPCR of resected tumor masses demonstrating on-target effects of miR-210 inhibition by

Targapremir-210. * Indicates $p < 0.05$ compared to untreated mice, as determined by a two-tailed Student *t* test.

Table 1

Secondary Structure of RNA Isoforms That Contain Fit Motifs for Targapremir-210, Listed with Associated Predicted Affinity for the Labeled RNA Motif (blue boxes)[a]

K_d, (nM)	Motif (5′/3′)	miRNA	Secondary Structure
165[b]	ACU/ACU	hsa-miR-210	
		hsa-miR-497	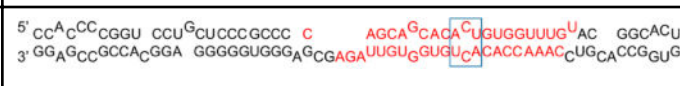
2500	UAU/ACA	hsa-miR-466	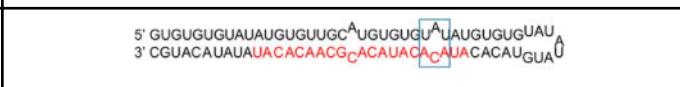
		hsa-miR-505	
		hsa-miR-140	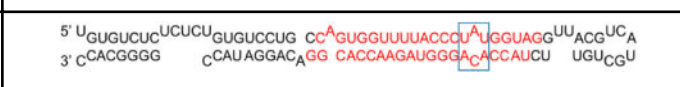
2900	AUU/UCA	hsa-miR-181a-2	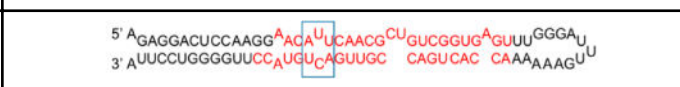
		hsa-miR-324	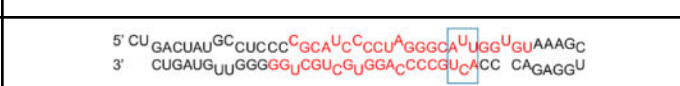
3700	CCU/GAA	hsa-miR-648	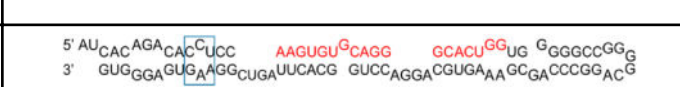
		hsa-miR-103a-1	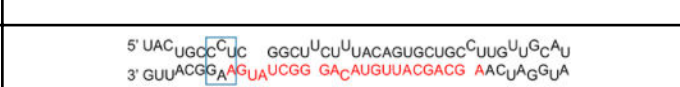
		hsa-miR-1273c	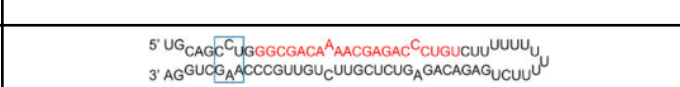
		hsa-miR-4682	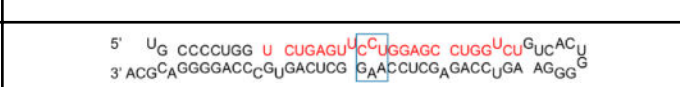
		hsa-miR-3120	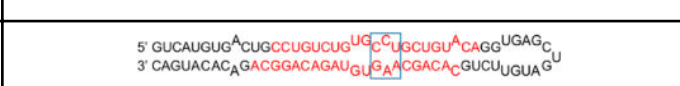
7900	AGC/UAG	hsa-miR-3174	
11000	UUU/ACA	hsa-miR-4446	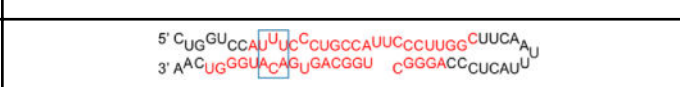
		hsa-miR-107	

K_d, (nM)	Motif (5′/3′)	miRNA	Secondary Structure
		hsa-miR-3613	

[a] Mature microRNA sequences are indicated in red.

[b] Measured affinity.